

ME615 Project Report

Aeroacoustic Simulations using Lattice Boltzmann Method

Kameswararao Anupindi *

School of Mechanical Engineering, Purdue University, West Lafayette, IN, 47906, USA

Lattice Boltzmann method (LBM) offers an alternative to the conventional simulation of fluid flows.^{1,2} In this approach Navier-Stokes equations are not solved rather the lattice Boltzmann equations (LBE) are solved in a mesoscopic limit thus enabling the numerical simulation of fluid flows. Navier-Stokes equations can be derived from LBE by applying Chapman-Enskog multiscale and small parameter expansion, so it establishes the theoretical basis to simulate continuum using LBE. In the present project a 2D LBM solver is developed in Fortran 90 programming language and applied to study benchmark problems such as initial sound pulse, monopole, dipole and quadrupole. The simulation results of monopole are compared to the analytical solution for establishing the accuracy of the present method. Sound radiation patterns obtained for monopole, dipole and quadrupole conform to the theoretical ones discussed in the acoustics text book.⁹ Also, a study of limiting frequencies of excitation and wavelength are conducted by keeping the grid resolution fixed.

Nomenclature

ρ	Macroscopic density	τ	Relaxation time
f_α	Particle distribution function	t	time
f_α^{eq}	Particle equilibrium distribution function	\mathbf{x}	Position vector
\mathbf{c}_α	Particle velocity vector	Ω_α	Collision operator
\mathbf{u}	Macroscopic velocity vector	ν	Viscosity
δt	Unit time in space of lattice	w_α	Lattice weights
δx	Unit length in space of lattice	c_s	Lattice sound speed
$DnQm$	n dimensional lattice with m degrees of freedom	α	Lattice particle, subscript
\hat{S}	Monopole amplitude	$\hat{\mathbf{D}}$	Dipole moment-amplitude-vector

I. Introduction

Lattice Boltzmann method (LBM) is emerging as a potential methodology for simulating fluid flow. LBM finds its roots in lattice gas automata (LGA). Individual particles are tracked in LGA methods where as in LBM a set of particles arranged in a symmetric lattice are used. In a microscopic approach to simulating fluid flow one solves the effect of particles on other particles. In a continuum approach the fluid particles are assumed to be packed abundant enough in a control volume that it can be approximated as a continuous field and leads to simulations using Navier-Stokes equations by various techniques such as finite difference, finite volume, finite element or spectral methods. A mesoscopic approach falls in between these two methodologies and by fine tuning certain parameters it can be tailored to simulate either of them. LBM is based on a mesoscopic approach, in which individual particles are not tracked rather a set of particles arranged in a structured lattice are simulated. The effect of particles inside the lattice on each other is represented using a collision operation. The collision operator that controls the rate of approach

*Graduate Research Assistant

of the particles to an equilibrium state are modeled with Bhatnagar-Gross-Krook single-relaxation-time approximation.^{1,6} Navier-Stokes equations can be derived from LBE by applying Chapman-Enskog multiscale and small parameter expansion, so it establishes the theoretical basis to simulate continuum using LBE. There are two types of LBM that have been used for aeroacoustic simulations, they are classical LBM (CLBM)^{4,5} and finite difference lattice Boltzmann method (FDLBM).³ CLBM is only second order accurate in both space and time, whereas FDLBM can be used to perform simulations with higher order accuracy by choosing appropriate spatial and temporal discretizations. In this project we focus only on classical LBM for all the simulations.

II. Literature Review

Recently, there has been a lot of interest in the scientific community in applying LBM to various fluid flow simulations. Articles on LBM by Chen et al.,¹⁰ and Luo et al.² provide a complete review of the state of the art in the LBM simulations. Primarily, LBM is a compressible approach but keeping the Mach number and the lattice velocities very low LBM can be used to simulate incompressible flows as well. A quick review of the published literature is described below segregated by the application area.

- **Direct Numerical Simulations:**

Chikatamarla et al.⁷ performed three-dimensional direct numerical simulations (DNS) of Kida vortex, a prototypical turbulent flow, using a higher-order LBM using D3Q41 lattice. They compare local and global turbulent statistical quantities to the results obtained with a spectral element solver and conclude that LBM is a promising alternative for DNS as it quantitatively captures the statistics of incompressible fluid turbulence.

- **Large Eddy Simulations:**

Dong et al.¹ performed LBM combined with LES to study the effects of sub-grid models on time correlations in decaying isotropic turbulence. Two sub-grid models, inertial-range (IR) consistent model and the classical Smagorinsky model are compared to the DNS results and they show that LBM sub-grid models yield an underestimation of the magnitude of the time correlation on different time intervals and on a variety of wave number modes, similar to NS sub-grid models. They also conclude that among classical Smagorinsky model and IR consistent sub-grid model the latter shows promising results on the prediction of the time-space correlations in turbulent flows accurately with different initial spectra considered.

Malaspinas et al.¹³ performed LES studies on temporal mixing layer using the approximate deconvolution model. They validate the new model on the turbulent, time developing mixing layer, and a very satisfactory agreement is found with the DNS results.

- **Aeroacoustic Simulations:**

Kam et al.¹¹ report simulation results of acoustic wave scattering using FDLBM. Two cases of incoming acoustic waves are considered for scattering problem by the authors; one is the case of a short wavelength, and the other has a relatively long wavelength compared with the characteristic dimension. Only short wavelength waves could be simulated with fairly good accuracy using this method.

Viggen¹² in his dissertation, applied LBM to simulate a range of acoustic problems such as point source to simulate cylindrical and plane waves, Doppler effect, diffraction and standing waves. He concludes that LBM could be suitable for simulating acoustics in complex flows, at ultrasound frequencies and very small spatial scales. Also, it was shown that LBM is not feasible at lower frequencies or for larger scales.

Lew et al.⁴ predicted the noise generated by a subsonic turbulent round jet in the far field using LBM. The near field flow results such as jet center line velocity decay rates, and turbulence intensities computed by LBM were found to be in good agreement with experimental and Navier-Stokes based LES simulations. Also, the far field sound pressure levels were within 2dB of the experimental results. They conclude that LBM seems to be a viable approach, comparable to LES in accuracy for the problem under consideration.

III. The Simulation Method

LBM is a numerical method for solving the Boltzmann equation (1), where $f_\alpha(\mathbf{x}, t)$ is a set of distribution functions, which represents the probability of finding a particular particle at a position \mathbf{x} at time t with a velocity \mathbf{c}_α .

$$f_\alpha(\mathbf{x} + \mathbf{c}_\alpha \delta t, t + \delta t) - f_\alpha(\mathbf{x}, t) = \Omega_\alpha \quad (1)$$

The collision operator Ω_α models the collision of particles and controls the rate of approach of distribution functions to an equilibrium state given by f_α^{eq} . Bhatnagar, Gross, and Krook⁸ proposed the BGK dynamics, where the collision operator Ω_α is approximated as a single-relaxation-time (SRT) model as given by equation. (2).

$$\Omega_\alpha = \frac{1}{\tau} [f_\alpha(\mathbf{x}, t) - f_\alpha^{eq}(\mathbf{x}, t)] \quad (2)$$

Where τ is the relaxation time related to the viscosity (ν) as follows:

$$\tau = \frac{3}{\delta t} \nu + \frac{1}{2} \quad (3)$$

The equilibrium distribution function $f_\alpha^{(eq)}$ is obtained by discretizing the Boltzmann distribution. In the present work the form given in equation (4) is used which involves terms in velocity up to second order,

$$f_\alpha^{eq}(\rho, \mathbf{u}) = w_\alpha \rho \left[1 + \frac{\mathbf{c}_\alpha \cdot \mathbf{u}}{c_s^2} + \frac{(\mathbf{c}_\alpha \cdot \mathbf{u})^2}{2c_s^4} - \frac{|\mathbf{u}|^2}{2c_s^2} \right] \quad (4)$$

with the lattice speed of sound $c_s = \frac{1}{\sqrt{3}}$ for the D2Q9 model and the lattice weights are given as follows:

$$w_{k=9} = 4/9 \quad (5)$$

$$w_{k=1,2,3,4} = 1/9 \quad (6)$$

$$w_{k=5,6,7,8} = 1/36 \quad (7)$$

and the lattice is defined by the following vectors as shown in equation (8), for $i = 1, 9$.

$$c_i = \begin{bmatrix} 1 & 0 & -1 & 0 & 1 & -1 & -1 & 1 & 0 \\ 0 & 1 & 0 & -1 & 1 & 1 & -1 & -1 & 0 \end{bmatrix} \quad (8)$$

The convention to define a lattice type is $DnQm$ where Dn denotes the dimension of the lattice with n set to 2 for 2D and 3 for 3D and Qm defines the number of lattice sites. For example $D2Q9$ lattice used in the present simulations is a 2D lattice and has 9 lattice sites or degrees of freedom.

The macroscopic observable quantities are given by the moments of the particle distribution function as follows. The integral of zeroth moment of distribution function gives the density and the first moment gives the momentum as described in equations (9,10).

$$\rho(\mathbf{x}, t) = \sum_{\alpha} f_\alpha(\mathbf{x}, t) \quad (9)$$

$$\rho(\mathbf{x}, t) \mathbf{u}(\mathbf{x}, t) = \sum_{\alpha} \mathbf{c}_\alpha f_\alpha(\mathbf{x}, t) \quad (10)$$

With this introduction to the numerical method we present the general algorithm to solve the LBM on a finite difference grid with a lattice attached to each of the grid point. The Algorithm to simulate using LBM consists of three main steps as described below.

A. Algorithm

1. Collision
2. Streaming
3. Boundary conditions

In the collision step the particle distribution function f_α are relaxed towards their respective equilibrium value $f_\alpha^{(eq)}$ according to equation (2). In the streaming step each f_α is *streamed*, or *advected* to the respective lattice site dictated by its lattice vector \mathbf{c}_α . The D2Q9 lattice is shown in Figure (1a) with the corresponding lattice vectors. The streaming operation is shown in Figure (1b). With this we can explain how the streaming/advection occurs which essentially represented on the left hand side of the equation (1). For example if we assume that the lattice in the center with all solid arrows in Figure (1b) is the location where streaming has to be performed, then the distribution function corresponding to each of the arrows/lattice sites are advected/streamed to the adjacent lattice as per the color coding and the final position where the distribution function is assigned is represented by the broken arrows. Similarly the rest of the arrows shown in black will also receive their values from their neighbors and so on. Care should be taken while doing streaming operation such that we do not stream same value all along. For e.g. if we use a copying mechanism then for copying the distribution function values for $C6$ on x -axis we should start at the x -max location first and march towards x -min location. If we do it other way round then the value of $C6$ at x -min gets copied to all the grid points because the distribution function at the next site gets over-written before they could be copied.

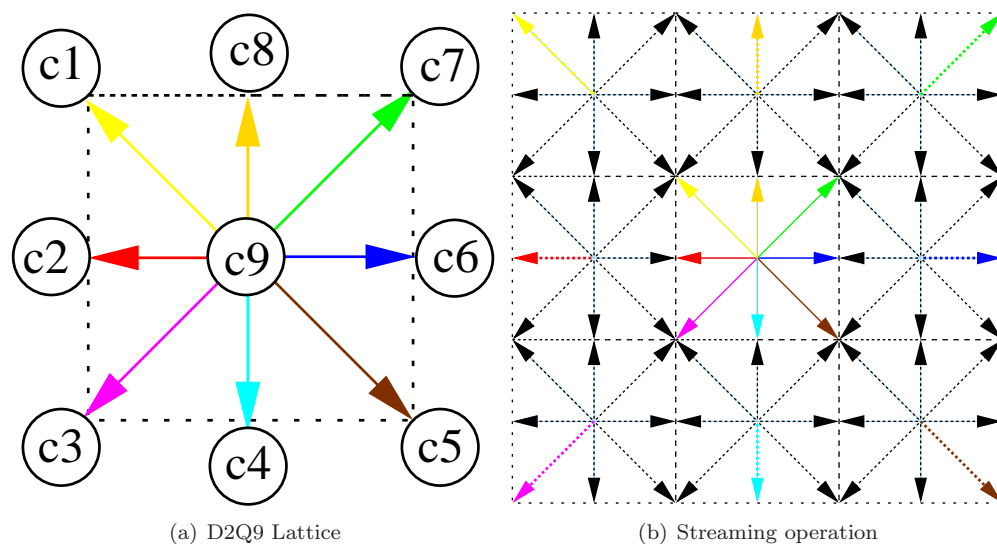


Figure 1. Schematic showing the lattice structure and streaming operation

B. Boundary conditions

In the present simulations periodic boundary conditions are used on all boundaries. These are the simplest type of boundary conditions. In this the outgoing distribution functions are set as incoming distribution functions on the other periodic boundary.

IV. Results

Various bench-mark problems in aeroacoustics are simulated here using the 2D LBM solver that was developed during the course of the project. In all the simulations the background velocity (u, v) is set to zero and density perturbation are imposed on a uniform density of $\rho_o = 1.0$. Then the evolution of the density perturbations are tracked and also there will be tiny velocities that get set up because of traveling density

waves in the domain. The off-equilibrium density or density perturbation ρ' is computed as $\rho' = \rho - \rho_o$. In LBM simulations the pressure turns out to be proportional to density as $p = c_s^2 \rho$. Therefore, one can compute pressure perturbations from the density perturbations using this relation and similarly we can write $p' = p - p_o$, where $p_o = c_s^2 \rho_o$.

In all the simulations we use periodic boundary conditions on the domain boundaries and the simulations times performed are less than the time required for the wave to leave the domain and re-enter from the other side. Also, the acoustic waves get damped before they reach one of the periodic boundaries. The domain extent is set to 100X100 and $\tau = 1.0$ was chosen.

A. Initial Pulse

First we test the code by using a simple test case in which a simple delta function in density is imposed on a uniform density field. At $t = 0$, the density field is set to $\rho = 1.0$ every where except at the center point (50,50) of the domain where we set $\rho = 1.1$. This initial density pulse now should propagate into the domain from its initial position with speed of sound. Because we set $\tau = 1$ the viscosity is fixed according to equation (3) and the density pulse should propagate according to the lattice speed i.e. with $c_s = 1/\sqrt{3} = 0.577$. The results obtained from the initial pulse case are shown plotted in Figure (2). The evolution of the density perturbation is shown in Figures (2a)-(e). We can see from these figures that the wave front travels outward in a circular pattern from the center. Figure (2f) shows the density fluctuation as a function of x at various time instants along $y = 0$ line. The extracted wave signals again reveal the property of traveling outwards from the center and this plot is used to calculate the speed of sound in this medium from the speed of the wave. For e.g. at $t = 10$ the right side peak of the wave is at $x = 56.54$, so it took $t = 10$ to travel a distance of $56.54 - 50.0 = 6.54$ giving a speed of sound of 0.654. Similarly the speeds calculated at times $t = 20, 30, 40$ equal 0.795, 0.633, 0.625 respectively. As we can see all the speed of sounds predicted are higher than the actual value of $c_s = 0.577$. For some reason the value at $t = 20$ has a higher value than the rest of the values.

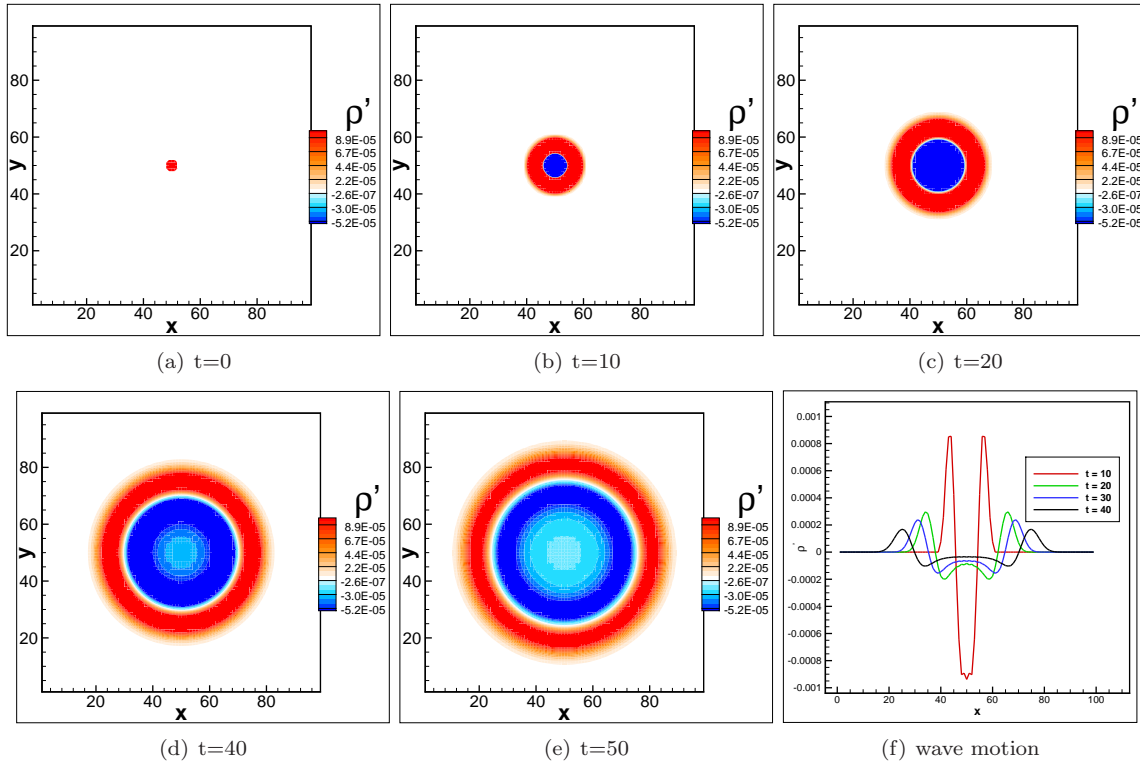


Figure 2. Propagation of density perturbation waves for the case of pulse

B. Monopole

A monopole can be generated by a radially oscillating sphere. In the present case to produce a field similar to that generated by a monopole the density of a particular point is locked so as to produce small perturbations in density in a quiescent fluid. The density field is perturbed continuously according to the following equation $\rho = \rho_o + \rho' \sin(2\pi t/T)$. The density at the center of the domain i.e. at $(x, y) = (50, 50)$ is locked to this value. Where $\rho_o = 1.0$, $\rho' = 0.01$, and $T = 20.0$. The evolution of the density perturbations from $t = 10$ to $t = 50$ are shown plotted in Figure (3a-e). As we can see from these plots the magnitude seen at the center of the domain is same at frames $t = 20$ and $t = 40$ because the wave has a period of $T = 20$. Also, the perturbations travel outwards from the center as can be seen from the plots. The same can be better visualized in Figure (3f) where the wave is extracted on $y = 0$ line and plotted at different times. In frames (g)-(i) of Figure (3) we compare the computed density perturbations to the analytic solution. These plots reveal that the wave length seems to be better captured by LBM but not the magnitude. This needs to be further investigated as to why the solution does not match perfectly. The analytical solution to the monopole is given by $p' = AH_0^{(2)}(kr)e^{i\omega t}$ where $k = \frac{\omega}{c_s}$ and $H_0^{(2)}$ is Hankel function given by $H_0^{(2)}(kr) = J_0(kr) - iY_0(kr)$, further J_0, Y_0 are Bessel functions of first, and second kind respectively. Using $A = 0.135\rho_s e^{-2\pi/3}$ for $T = 20$ and $c_s = 1/\sqrt{3}$ the exact or the analytical solution shown in Figure (3) was calculated.

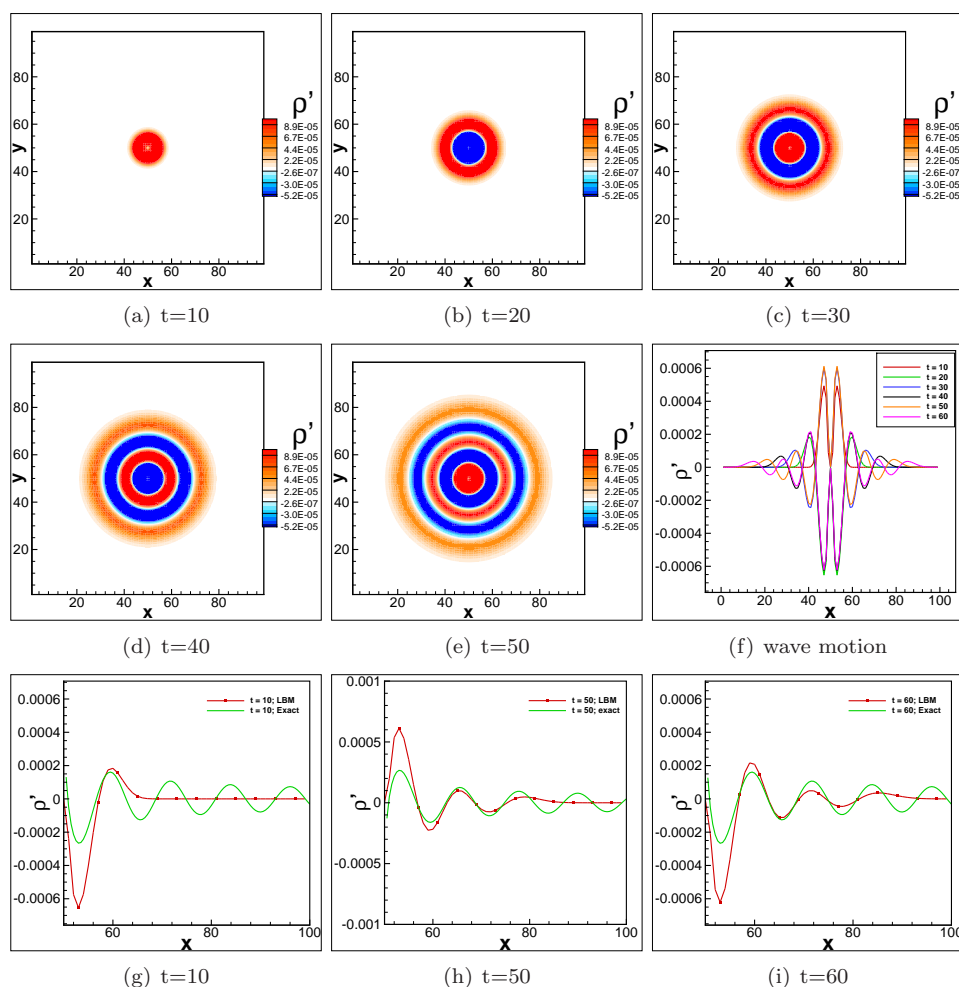


Figure 3. Propagation of density perturbation waves for the case of monopole

Next, we performed a study by varying the time period of oscillations. The time period of excitation was varied from $T = 1$ to $T = 100$ and the density perturbation is shown plotted for these cases in Figure (4) at simulation time of $t = 60$. As we can see from Figure (4), $T = 1$ does not seem to be captured by the

current grid which has $\delta x = 1, \delta t = 1$. Where as $T = 5$ shows one wave length of perturbation and then damps out. Larger excitation periods such as $T = 10$ and $T = 20$ show at least two wave lengths before they damp out. And much higher excitation periods as $T = 50$ and $T = 60$ again show only one wave length. Highest excitation period considered in this case was $T = 100$ and the present grid with the simulation time of $t = 60$ could not capture even a single wave length. So we can conclude that moderate time periods of excitation considered here such as $T = 10$ or $T = 20$ seem to be ideal candidates for the simulations on the resolution considered. Both extremes such as $T = 1$ and $T = 100$ need much finer δt or longer domain sizes respectively to be captured properly.

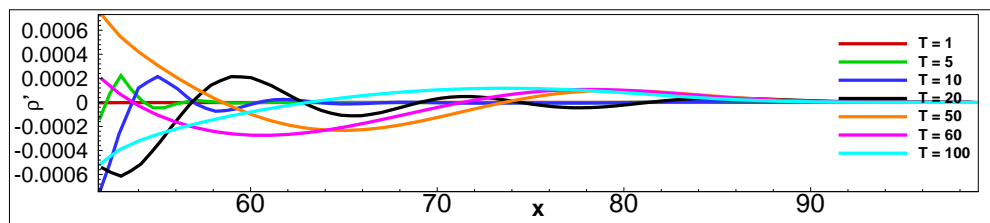


Figure 4. Propagation of density perturbations for different time periods of excitation

C. Dipole

Having simulated the monopole case, we further perform simulation of a dipole. A dipole in practice could be generated by a transversely oscillating sphere. In other words, a dipole can be thought of as a superposition of fields of two or more monopoles located at different points.⁹ We use here two point sources each described by the monopole perturbations of amplitudes \hat{S} and $-\hat{S}$, that is, 180° out of phase with each other, and located a distance $d = 2\delta x$ apart. The density perturbations generated by such a dipole field are simulated and shown in Figures (5a-e). Also, waves extracted from $y = 0$ plane are shown plotted in Figure (5f). From these plots we can observe that unlike a monopole field which produced circular waves emanating outwards from the center, out of phase waves are emitted at the center propagate canceling their effect on the $x = 0$ plane. Hence an observer located here will not perceive the sound radiated by a dipole field.

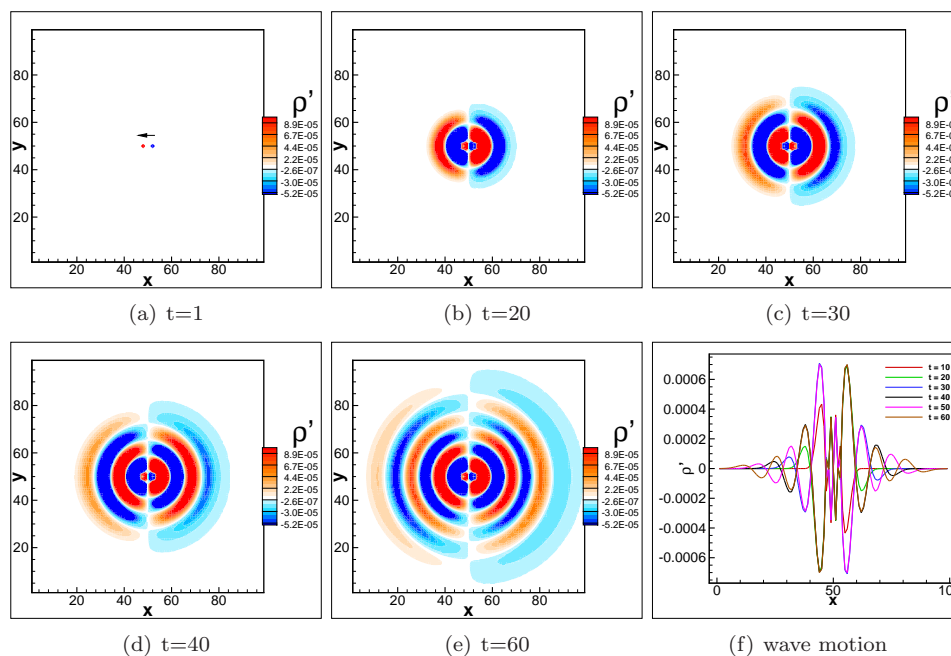


Figure 5. Propagation of density perturbation waves for the case of a dipole

D. Quadrupole

Next, we simulate quadrupole using the LBM solver. A quadrupole as the name suggests can be conceptualized as two closely spaced dipoles, with equal but opposite dipole-moment amplitude vectors $\hat{\mathbf{D}}$. In the present simulations we simulate both a longitudinal and lateral quadrupole. Depending on whether the line joining the dipoles \mathbf{d} is parallel or perpendicular to the dipole-moment-amplitude vector $\hat{\mathbf{D}}$ we can call it a longitudinal or a lateral quadrupole. The same can be seen plotted in frame (a) of Figures (6, 7).

1. Longitudinal Quadrupole

In the longitudinal quadrupole simulations the \mathbf{d} is set to $2\delta y$ and the results obtained are shown plotted in Figures (6a-e). The waves are extracted on $x = 0$ line and are shown in Figure (6f). The solution obtained for the longitudinal quadrupole seems qualitatively similar to the one of dipole. The radiation wave pattern obtained is similar to what is described in the text book,⁹ we can see that an eight-shaped pattern is obtained.

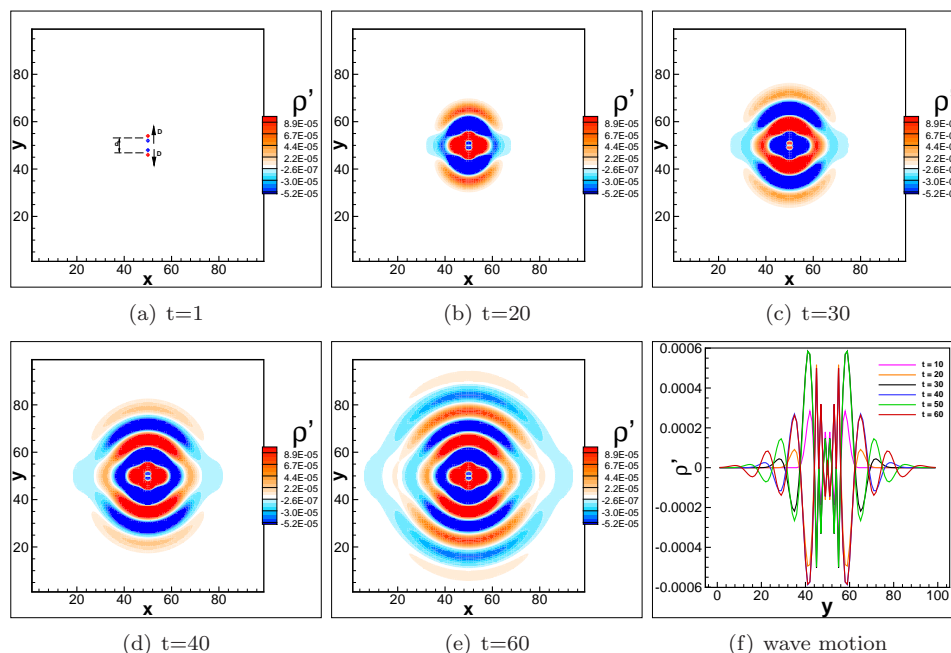


Figure 6. Propagation of density perturbation waves for the case of a longitudinal quadrupole

2. Lateral Quadrupole

A lateral quadrupole is formed when the dipole-moment-amplitude-vectors $\hat{\mathbf{D}}$ are perpendicular to the line joining the dipoles \mathbf{d} . Figure (7) shows the density perturbations at indicated times, and in frame (f) of Figure (7) we show the extracted wave motion on $x = y$ line. The acoustic radiation pattern obtained is similar to what is expected for a lateral quadrupole which should be like two eight-shaped figures arranged perpendicular to one another.

V. Conclusion

In this project we developed a 2D LBM solver in Fortran 90, that can simulate fluid flow and acoustic problems. The developed solver was applied to simulate a variety of bench-mark problems in aeroacoustics such as an initial sound pulse, a monopole, dipole, and both longitudinal and lateral quadrupole. The simulation results seem to be qualitatively matching to the ones shown in theory. However, an exact match is not achieved for the sound speed and to the analytic solution for the monopole case that were considered. This could be related to the difference in sound speed predicted, and further investigation needs to be performed. The radiation patterns produced by all the bench-mark cases are similar to those described in

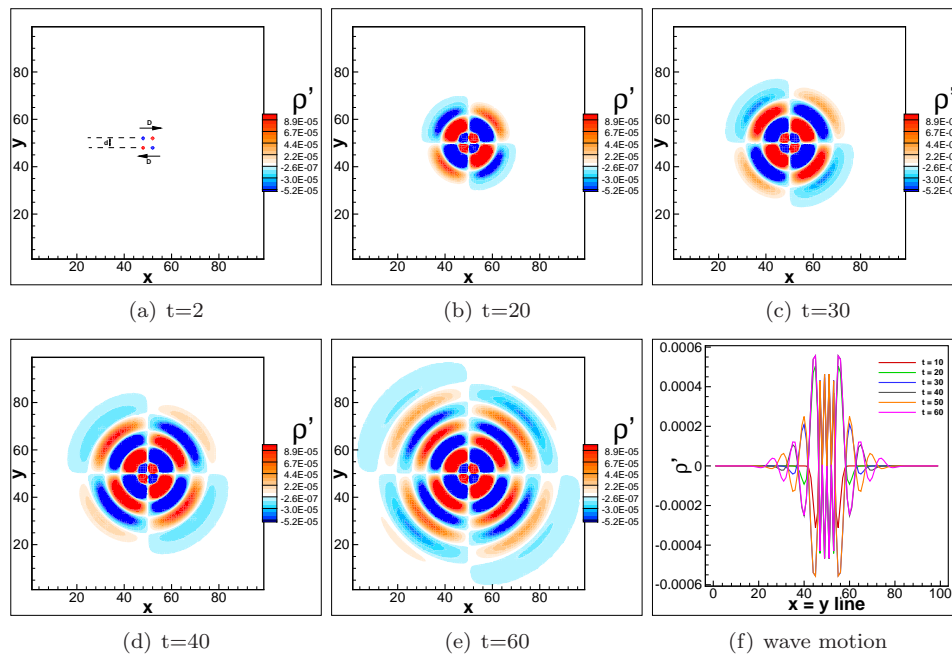


Figure 7. Propagation of density perturbation waves for the case of a lateral quadrupole

theory in the text book.⁹ A study on the time period of excitation for the monopole case was performed and it is found that moderate time periods such as $T = 10$ and $T = 20$ are better resolved by the grid resolution considered. In conclusion, lattice Boltzmann method seems to be a viable alternative approach to simulate fluid flow and acoustics.

VI. Appendix

A. Code Snippets

Here couple of code snippets are shown from the 2D LBM Solver. The following shows the main program.

```

program LatticeBoltzmann2D
  use lbm_memory
  implicit none

  call read_input_file()

  call allocate_lbm_memory()

  call initialize_lbm()

  call solve_lbm()

  call deallocate_lbm_memory()

end program LatticeBoltzmann2D

```

The code below is the solve_lbm subroutine that performs the main solution loop.

```
subroutine solve_lbm()
  implicit none

  do step = 1, nsteps

    call collision()
    call periodic_bc()
    call streaming()
    call compute_primitive_variables()

    write(*, '(i10, 5x, f25.15, 5d, f25.15, 5x, f25.15)') , step, sum(u(:, :)), sum(v(:, :)), ←
      sum(rho(:, :))

    if (mod(step, 5) == 0 .or. step == 1) then
      call output_tecplot(step)
    end if

  end do

end subroutine solve_lbm
```

References

- ¹Dong, Y., and Sagaut, P., *A study of time correlations in lattice Boltzmann-based large-eddy simulation of isotropic turbulence*, Physics of Fluids, **20**, 035105 (2008).
- ²Luo, L., Krafczyk, M., and Shyy, W., *Lattice Boltzmann method for Computational Fluid Dynamics*, Encyclopedia of Aerospace Engineering, John Wiley & Sons, Ltd.
- ³Hiraishi, M., Tsutahara, M., and Leung, R., C., K., *Numerical simulation of sound generation in a mixing layer by the finite difference lattice Boltzmann method*, Computers and Mathematics with Applications, **59**, 2403-2410 (2010)
- ⁴Lew, P., T., Mongeau, L., and Lyrantzis, A., *Noise prediction of a subsonic turbulent round jet using the lattice-Boltzmann method*, Journal of the Acoustical Society of America, **128(3)**, 1118-1127 (2010)
- ⁵Li, X., M., Leung, R., C., K., and So, R., M., C., *One-Step Aeroacoustics Simulation Using Lattice Boltzmann Method*, AIAA Journal, **44**, No. 1, (2006)
- ⁶Ricot, D., Marié, S., Sagaut, P., and Bailly, C., *Lattice Boltzmann method with selective viscosity filter*, Journal of Computational Physics, **228**, 4478-4490, (2009).
- ⁷Chikatamarla, S., S., Frouzakis, C., E., Karlin, I., V., Tomboulides, A., G., and Boulouchos, K., B., *Lattice Boltzmann method for direct numerical simulation of turbulent flows*, Journal of Fluid Mechanics, **656**, 298-308, (2010).
- ⁸Bhatnagar, P. L., Gross, E., P., and Krook, M., *A Model for Collision Processes in Gases. I. Small Amplitude Processes in Charged and Neutral One-Component Systems*, Physical Review, **94(3)**, 511-525, (1954)
- ⁹Pierce, A. D., *Acoustics, An Introduction to Its Physical Principles and Applications*, **Acoustical Society of America**, (1994)
- ¹⁰Chen, S., and Doolen, G., D., *Lattice Boltzmann Method for Fluid Flows*, Annual Review of Fluid Mechanics, **30**, 329-364, (1998)
- ¹¹Kam, E., W., S., So, R., M., C., Fu, S., C., and Leung, R., C., K., *Finite Difference Lattice Boltzmann Method Applied to Acoustic-Scattering Problems*, AIAA Journal, **48(2)**, (2010)
- ¹²Viggen, E., M. *The Lattice Boltzmann Method with Applications in Acoustics*, Masters Dissertation, Department of Physics, NTNU (2009)
- ¹³Malaspinas, O., and Sagaut, P., *Advanced large-eddy simulation for lattice Boltzmann methods: The approximate deconvolution model*, Physics of Fluids, **23**, 105103 ,(2011)